Stopping powers of havar for 0.63–5.9 MeV protons and 2.6–24 MeV alpha particles

2004 J. Phys.: Condens. Matter 16 7663

(http://iopscience.iop.org/0953-8984/16/43/009)

INSTITUTE OF PHYSICS PUBLISHING JOURNAL OF PHYSICS: CONDENSED MATTER

J. Phys.: Condens. Matter **16** (2004) 7663–7672 PII: S0953-8984(04)80120-6

Stopping powers of havar for 0.63–5.9 MeV protons and 2.6–24 MeV alpha particles

L E Porter[1], W H Trzaska[2], J Räisänen[2,3] and V Lyapin[2]

[1] Washington State University, Pullman, WA 99164-1302, USA
[2] University of Jyväskylä and Helsinki Institute of Physics, PO Box 35, FIN-40014 Jyväskylä, Finland

E-mail: porterl@wsu.edu

Received 5 May 2004, in final form 9 August 2004
Published 15 October 2004
Online at stacks.iop.org/JPhysCM/16/7663
doi:10.1088/0953-8984/16/43/009

Abstract

A transmission experiment utilizing thin foil targets has been conducted in order to establish the stopping powers of the cobalt-base alloy, havar, for 0.6–5.9 MeV protons and 2.6–24 MeV alpha particles. The basic technique of the novel experimental method used was to record both the projectile energy and the time of flight while alternating measurements with and without the target in place. The uncertainties of the proton and alpha particle data sets ranged from 1.4 to 2.3% and 1.1 to 1.5%, respectively. Modified Bethe–Bloch theory was applied to the measurements in order to ascertain values of the target mean excitation energy (I) and Barkas-effect parameter (b) for each projectile. The extracted values were $I = 304.3 \pm 2.4$ eV and $b = 1.37 \pm 0.04$ for the case of protons, and $I = 306.3 \pm 2.3$ eV and $b = 1.47 \pm 0.03$ for the case of alpha particles. The I-values are somewhat higher than the additivity-based expectation of 295.7 eV, whereas the b-values are clearly consistent with the expected range of 1.4 ± 0.1. The parameter values extracted from the measurements are appraised for compatibility with recently observed trends in values of I and of b with increasing projectile atomic number.

(Some figures in this article are in colour only in the electronic version)

1. Introduction

During the past century a topic that has proved both challenging and intriguing to theoretical physicists is the stopping power of matter for charged particles. The topic has retained the vital interest of those in numerous areas of basic and applied physics who needed to know quite accurately the energy loss of a charged subatomic particle in traversing a given

[3] Present address: Department of Physical Sciences, University of Helsinki, Accelerator Laboratory, PO Box 43, FIN-00014 Helsinki, Finland.

thickness of a specific target material. When that need could not be met by any extant theory sufficiently developed to possess a reliable predictive capability, measurements were conducted with the specified target material and one or more projectiles. One approach that has served for calculation of the energy loss over a broad interval of projectile velocities above about 0.5 MeV u^{-1} is the modified Bethe–Bloch theory of stopping power, provided that values of several parameters of the formalism have been established [1–5]. In the event that the target possesses aggregation effects, as in the case of compounds and alloys in particular, one method of managing the complexity of the situation is to invoke Bragg's rule [6], which assumes the linear additivity of stopping effects. The technique utilized for the calculation of energy loss in this type of target has been described in several previous studies [1–5].

A continuing focus of interest for one of the authors (LP) over nearly the past four decades [7, 8] has been the alloy called havar[4]. The first reported study of stopping power by this author described both a set of measurements and analysis [8]. Measurements with light projectiles were summarized two decades later [9], and two of the current authors (LP and JR) joined in an investigation of physical state effects on the stopping powers of havar for protons and alpha particles [4]. The current study considerably extends the energy intervals covered for the same projectiles, incorporating a new experimental method [10, 11]. Previous measurements of the stopping powers of havar for several heavy ions [12] are not analysed in this investigation, which is focused on light projectiles.

2. Experiment

The present measurements with the alloy, havar, are a continuation of our previous study in which the stopping powers of protons and alpha particles for polycarbonate were determined [11]. The experimental arrangement is the same as in that study, as reported in detail in [10] and [13]. A test of the method employed for reliability and accuracy is included in the references. In brief, both the energy and the time of flight (TOF) of the ions are recorded while constantly alternating between measurements with and without the havar foil inserted in the ion beam. The time of flight is determined by a TOF spectrometer before the ions pass through the havar foil and the ion energy is determined after traversing the foil by a solid state detector. The events recorded with and without the foil can be matched, and the data points thus obtained form two curves on a two-dimensional plot with energy and TOF as the axes. By comparing the energy values at the corresponding TOF values one obtains a set of energy loss data points that are equivalent to several individual step-by-step conventional transmission type measurements.

The stopping medium was a single foil with nominal thickness of 2.4 μm supplied by Hamilton Precision Metals of Lancaster, PA. The precise areal density was determined by weighing a circular piece (20 mm diameter) of the foil. The material thickness uniformity was checked by energy loss measurements from several spots on the foil employing a collimated ^{226}Ra alpha source. The havar foil properties provided in table 1 were obtained from the technical office [14] of the supplier (see footnote 4). The uncertainties in concentrations are those implied by the significant figures as given. The 0.5% error assigned for the foil areal density (1.845 ± 0.010 mg cm^{-2}) includes uncertainties arising from the foil area determination, weighing, and a non-uniformity study.

The total ion fluence on the havar target foil was kept below 10^7 particles cm^{-2}. This low limit on fluence ensures no alteration of the alloy properties such that the deduced stopping power values would be affected.

[4] Havar is a cobalt-base alloy supplied by Hamilton Precision Metals of Lancaster, PA 17604-3014, USA.

Table 1. The nominal composition and specific density (ρ) of the havar material studied.

	Element	Concentration (at.%)
	Be	0.3
$\rho = 8.30$ g cm^{-3}	C	1.0
	Cr	22.2
	Mn	1.7
	Fe	18.1
	Co	41.6
	Ni	12.8
	Mo	1.4
	W	0.9

Table 2. Experimental stopping power values of havar for protons.

E_{avg} (MeV) proton	S (keV cm^2 mg^{-1})	ΔS (keV cm^2 mg^{-1})	Relative error $\Delta S/S$ (%)	$\Delta E/E_{avg}$ (%)	Number of events
0.632	163	2.3	1.4	47.6	71
0.710	153	2.2	1.4	40.0	524
0.856	138	1.9	1.4	29.9	967
1.025	125	1.8	1.5	22.6	1 607
1.227	112	1.6	1.4	16.9	2 795
1.461	101	1.5	1.5	12.8	4 809
1.732	92	1.4	1.5	9.8	7 820
2.038	83	1.3	1.5	7.5	12 631
2.374	75	1.2	1.6	5.9	19 321
2.737	69	1.0	1.5	4.6	25 956
3.119	63	1.0	1.6	3.7	25 310
3.634	57	0.9	1.6	2.9	16 369
5.899	41	0.9	2.3	1.3	50 000

The stopping power at the mean ion energy (E_{avg}) in the foil was calculated by dividing the energy loss (ΔE) by the foil areal density ($\rho_{areal} = \rho \Delta x$), where ρ is the mass density of havar and Δx is the foil thickness. The mean ion energy is defined as $E_{avg} = E_i - \Delta E/2$, where E_i is the incident ion energy. In principle, nonlinear energy dependence of the stopping power introduces a small shift in the value of E_{avg}. In the present experiment the magnitude of that correction was always less than 1%, so the stopping power, $S = -(1/\rho)(dE/dx)$ (differential energy loss per unit path length), could be taken as $\Delta E/\rho \Delta x$ at the mean ion energy, E_{avg}.

The main sources of uncertainty in the deduced stopping power values are the areal density of the foil and the ion energy determination. In the stopping power values given in tables 2 and 3 these error sources have been taken into account. The energy calibration was carried out using a ^{226}Ra source and the position in the energy spectrum of the beam scattered from a thin target. The results were compared with the TOF-based values using the absolute time calibration of the TOF spectrometer. The consistency between the two approaches was within 1% for alpha particles and 2% for protons. For the final results the TOF calibration was used, since it is not sensitive to possible pulse height defects. (For a detailed discussion of this topic, see [10].) The statistics of the collected events were very good. The only exceptions can be found just below the highest energy point where, due to the small energy loss (<0.5%), the statistics of about 10^4 experimental events were not quite satisfactory. (The situation could have been improved by using longer collection times for the data, but the available beam

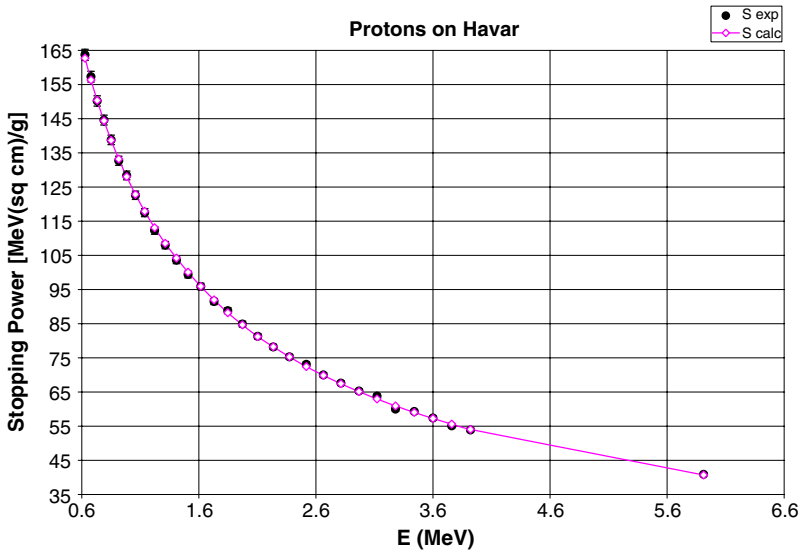

Figure 1. Comparison of experimental values of the stopping power of havar for protons (solid circles) with calculated values (open diamonds), in a two-parameter fit for the mean excitation energy (I) and Barkas-effect parameter (b).

Table 3. Experimental stopping power values of havar for alpha particles.

E_{avg} (MeV) alpha	S (keV cm^2 mg^{-1})	ΔS (keV cm^2 mg^{-1})	Relative error $\Delta S/S$ (%)	$\Delta E/E_{avg}$ (%)	Number of events
2.656	634	7	1.1	41.4	2 034
2.985	598	7	1.1	37.3	6 333
3.503	550	6	1.1	31.0	8 098
4.083	505	6	1.1	25.5	10 139
4.729	465	5	1.1	20.8	11 935
5.440	427	5	1.1	17.0	13 529
6.207	394	5	1.2	13.8	14 584
7.023	365	4	1.2	11.1	15 150
7.878	339	4	1.2	9.0	15 662
8.762	317	4	1.1	7.2	15 177
9.664	299	4	1.2	5.8	14 287
10.578	279	3	1.2	4.6	12 441
11.491	265	3	1.2	3.7	9 591
12.400	252	3	1.0	3.0	5 486
13.213	249	3	1.0	2.4	1 913[a]
15.763	222	2	1.1	1.5	2 164[a]
23.823	161	2	1.5	0.9	118 700

[a] Poor statistics. Too few counts per energy unit.

time was definitely limited.) Special attention should be given to the reference data points at the highest energies in figures 1 and 2. These points possess very good accuracy because they are based on measurements employing a very thin scatterer to obtain a monoenergetic beam that were conducted solely for the purpose of establishing these data points. (Please see [10] and [13].) It should be noted that in contrast, at the low energy end of the energy interval covered, where there was an energy loss of about 30%, even fewer than 100 events

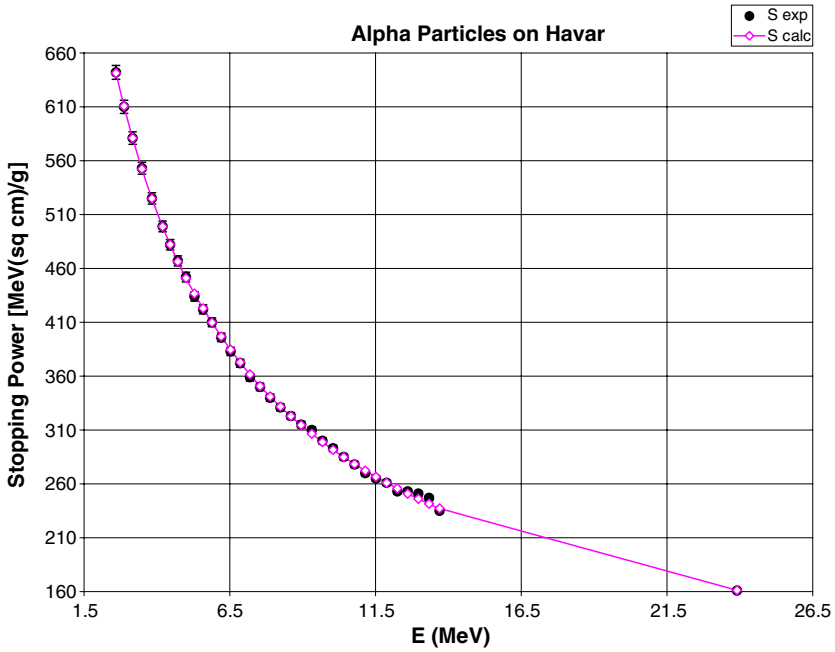

Figure 2. Comparison of experimental values of the stopping power of havar for alpha particles (solid circles) with calculated values (open diamonds), in a two-parameter fit for the mean excitation energy (I) and Barkas-effect parameter (b).

are sufficient for a reliable data point. The total number of events on which each experimental point is based is listed in tables 2 and 3. It should be noted that the data in tables 2 and 3 represent selected subsets of the complete data files, each constituting about 22% of the total number of data points determined.

3. Theory

The proper current theory of the stopping power of a specified target material for projectiles possessing velocities sufficiently high to preclude gain and loss of electrons while traversing the target is provided by the Bethe–Bloch formula modified by a Barkas-effect term. The formula features several target-specific parameters, of which a majority generally have values independent of the projectile velocity. Furthermore, most of these parameters cannot be calculated from first principles except for very light elemental targets, necessitating fits to experimental data for evaluation. A rather cursory presentation of the basic Bethe–Bloch formula will be followed by discussion of the important modifications represented by inclusion of the Barkas-effect and Bloch terms added just three decades ago, an effective charge formalism, and adaptation of the formula to target materials manifesting aggregation effects.

The stopping power of an elemental target with atomic number Z, atomic weight A, and stopping number L can be calculated in units of keV cm^2 mg^{-1} for a projectile with atomic number z and velocity $v = \beta c$ according to the Bethe–Bloch formula:

$$S = \frac{0.307\,06}{\beta^2} z^2 \frac{Z}{A} L. \tag{1}$$

The (dimensionless) stopping number per target electron, L, contains three terms:

$$L = L_0 + zL_1 + L_2. \tag{2}$$

In this sum L_0 represents the basic stopping number

$$L_0 = \ln\left(\frac{2mc^2\beta^2}{1-\beta^2}\right) - \beta^2 - \ln I - C/Z. \tag{3}$$

Here mc^2 denotes the rest mass energy of the electron, I is the mean excitation energy of the target element, and C represents the sum of target shell corrections.

L_1 signifies a Barkas-effect correction term. The term selected on the basis of a comparison of several versions of this term [15] is that which clearly provides superior agreement with measurements in general, the Ashley–Ritchie–Brandt version of the term [16–19]. Thus

$$L_1 = \frac{F(b/x^{1/2})}{Z^{1/2}x^{3/2}}, \tag{4}$$

where F denotes a function calculated and tabulated in [16], b constitutes the sole free parameter of the formalism [16–19], and $x = 18\,787\beta^2/Z$. L_2 is the Bloch correction term [20] resurrected by Lindhard during an investigation of higher order z-terms [21]:

$$L_2(y) = \psi(1) - \mathrm{Re}[\psi(1+\mathrm{i}y)], \tag{5}$$

where ψ is the digamma function [22] and $y = z\alpha/\beta$ with α representing the fine structure constant. The correction terms, L_1 and L_2, of L have been reviewed in conjunction with a random-phase evaluation of the first of these terms [23]. Shell corrections were obtained from the rubric of Bichsel [1] wherein C is calculated from a sum of contributions from the various shells,

$$C = C_{\mathrm{K}}(\beta^2) + V_{\mathrm{L}}C_{\mathrm{L}}(H_L\beta^2) + V_{\mathrm{M}}C_{\mathrm{L}}(H_{\mathrm{M}}\beta^2) + V_{\mathrm{N}}C_{\mathrm{L}}(H_N\beta^2). \tag{6}$$

In this expression C_i denotes the correction for the ith shell ($i = \mathrm{K}, \mathrm{L}, \mathrm{M}, \mathrm{N}$) and V_i and H_i are the corresponding scaling parameters. C_{K} and C_{L} were taken from those calculated by Walske [24, 25].

A complete set of parameters characteristic of a specified target comprises the target mean excitation energy, I, the shell correction scaling parameters, V_i and H_i ($i = \mathrm{K}, \mathrm{L}, \mathrm{M}, \mathrm{N}$), and the free parameter of the Barkas-effect correction term, b. (It must be noted that in the case of highly relativistic projectiles, a density effect correction term [26] must be added to L_0 and a second term [27] must be added to L_1.) All of the above parameters utilized in the present study are independent of both projectile velocity and a presumably constant projectile charge. However, when projectile energies considered are low enough to permit the gain and loss of electrons by projectiles travelling at velocities comparable to those of atomic electrons in the target, a projectile effective charge formalism must be employed to simulate the results of gain and loss of electrons. The technique used is the representation of the projectile charge (ze) by an 'effective charge' defined as (γze), where

$$\gamma = 1 - \zeta \mathrm{e}^{-\lambda v_{\mathrm{r}}}. \tag{7}$$

The symbol v_{r} stands for the ratio of projectile velocity in the laboratory frame of reference (v) to the Thomas–Fermi velocity $(2\pi e^2/h)z^{2/3}$, so $v_{\mathrm{r}} = \beta/\alpha z^{2/3}$. The symbols, λ and ζ, which denote the effective charge parameters over the entire projectile velocity interval considered, must be evaluated for any given projectile–target combination [28].

The preceding discussion pertains to an elemental target. The basic theories of Bohr and Bethe originally applied strictly to pure monatomic targets in the gaseous state [29]. However, a target material as simple as an elemental target in the condensed state, or as a homonuclear diatomic molecule in the gaseous state, is subject to bonding effects. The case of many atoms interacting simultaneously with a projectile and each other was first treated by Fermi as the 'density effect' [30]. It was Fano who explained the connection between the Bethe and

Fermi theories [29, 31] and subsequently described how the Bethe theory can be adapted to molecules and condensed matter [29]. Both physical state effects and chemical bonding effects are conventionally grouped together as aggregation effects. Procedures for calculating average parameter values have been described [16, 32], and the selection of mean excitation energy (I) and Barkas-effect parameter (b) as additivity test parameters has been explained [2]. The average (Bragg) value of the former, I_{B}, can be calculated [32] as

$$\ln I_{\mathrm{B}} = \sum_j n_j Z_j \ln I_j \Big/ \sum_j n_j Z_j, \tag{8}$$

where n_j, Z_j, and I_j denote respectively the atomic concentration, atomic number, and mean excitation energy of the jth component of the composite target material. The anticipated value of the Barkas-effect parameter, characterized by a very weak dependence on the target atomic number [16–18], is essentially the same as that of any constituent element (and especially so in the case of a compound consisting entirely of low Z elements). Thus the expected value of this parameter [19] is 1.4 ± 0.1 for essentially all target materials.

4. Method of analysis

The analysis of a set of stopping power measurements taken in the energy interval of applicability of modified Bethe–Bloch theory for a given projectile is conducted in accordance with a procedural strategy developed over the course of the previous three decades [2–5, 9, 29]. The formalism contains several target-dependent parameters, i.e., the mean excitation energy, the shell correction scaling parameters, and the Barkas-effect parameter, all of which are presumably independent of projectile charge, mass, and velocity. Shell correction scaling parameters could serve as searched parameters in an analysis but shell corrections represent a relatively small fraction of the total stopping number. Hence a fit to measurements would generally show little sensitivity to appreciable changes in the values of these parameters. In the stopping number the most dominant parameter by far is the target mean excitation energy, and the two parameters selected for evaluation from fits to measurements are the mean excitation energy (I) and the Barkas-effect parameter (b). Occasionally one or both effective charge parameters are established in analyses, with the proviso that even the most accurate data, high in density of measurements over the given projectile energy interval, rarely support the extraction of as many as three parameters. The figure of merit used in this fitting procedure is the root mean square relative deviation of calculated from measured stopping powers, σ. This quantity is defined as

$$\sigma = \sqrt{\frac{1}{N}\sum_{i=l}^{N}\left(\frac{S_{\mathrm{m}} - S_{\mathrm{c}}}{\Delta S_{\mathrm{m}}}\right)_i^2} \tag{9}$$

for measurements at N energies, with S_{m} denoting the measured stopping power, S_{c} the calculated stopping power, and ΔS_{m} the uncertainty in the measured value. Agreement between theory and experiment is indicated by a value of σ near unity.

The alloy, havar, was found to have values of average atomic number ($\overline{Z}$) and average atomic weight ($\overline{A}$), based on the composition of elements displayed in table 1, as shown in table 4. The values of the shell correction scaling parameters (H_{L}, V_{L}, H_{M}, V_{M}) are also displayed, as is the additivity-based (Bragg) value of the mean excitation energy (I_{B}), calculated from equation (8) with constituent I-values from [1]. With these values established, analyses of experimental data were conducted for the evaluation of the mean excitation energy (I) and Barkas-effect parameter (b). The projectile energy intervals employed precluded the necessity for inclusion of any effective charge parameter.

Table 4. The average atomic number ($\overline{Z}$) and atomic weight ($\overline{A}$), shell correction scaling parameters (H_L, V_L, H_M, V_M), and average target mean excitation energy (I_B) for the havar foil studied.

$\overline{Z}$	$\overline{A}$	I_B (eV)	V_L	H_L	V_M	H_M
26.6	57.8	295.7	1.00	1.00	1.88	7.13

Table 5. Results of initial fits to measurements with each light projectile, including the energy interval covered (E), the mean excitation energy (I), the Barkas-effect parameter (b), and the figure of merit (σ).

Study	Projectile	E (MeV)	I (eV)	b	σ
Current	Protons	0.63–5.9	304.3	1.37	0.41
Current	Alpha particles	2.6–24	306.3	1.47	0.90
Reference [4]	Protons	0.5–2.4	300.1	1.34	0.78
Reference [4]	Alpha particles	1.2–1.8	290.1	1.60	1.07

5. Results of analysis

Measurements for proton energies greater than 0.6 MeV were given a two-parameter fit in order to ascertain best-fit values of target mean excitation energy (I) and the Barkas-effect parameter (b). The energy interval selected, 0.63–5.9 MeV, featured a density of data points so large that two separate files covering the interval were prepared for ease of analysis. Each of the two files, selected by taking every other data point, was independent except that the highest energy point was included in each file. This inclusion was based on a gap in the measurements from 3.9 to 5.9 MeV. Similarly, two separate data files were prepared for alpha particle measurements above 2.6 MeV, covering the interval 2.6–24 MeV. In the alpha particle case a data gap existed from 13.9 to 23.9 MeV, so the highest energy point was common to both files.

Extracted values of I and b were averaged over the two files for each projectile, with results as shown in table 5. There was very little difference in the results for either of the two data files studied in the case of either light projectile. In comparison with the results of measurements for the same target and projectiles reported nearly a decade ago [4], the I-values for the two projectiles were much closer to one another in the present study (2.0 eV) than in the previous case (10.0 eV), as were the b-values (0.10 versus 0.26, respectively). In retrospect, the energy interval featured in the alpha particle measurements in the previous study [4] suggests that an effective charge parameter could have been included in the analysis. The fit for one of the data files for protons is displayed in figure 1, whereas the fit for one of the data files for alpha particles is displayed in figure 2. The excellence of fit reflected by the figure of merit for each case can be readily observed in the graphs. Furthermore, the values of the two parameters, I and b, are remarkably consistent with expectation, since the I-value exceeds the Bragg value (I_B) by 8.6 eV (2.9%) for protons and 11.1 eV (3.8%) for alpha particles. Moreover, the two values of b lie within the expected interval of values [19] of 1.4 ± 0.1. Finally, the current measurements for both projectiles are in remarkably close agreement with the predictions of SRIM 2003 [33], as illustrated in figure 3.

A matter of considerable interest is the uncertainties in the extracted values of I and b thus far established. These uncertainties will reflect the number and accuracy of the measurements, of course. A method for realistic calculation of these uncertainties was devised and described previously [4, 28]. In the present study that method was employed for the two-parameter fits, the results of which are shown in table 5. The uncertainties are displayed in table 6.

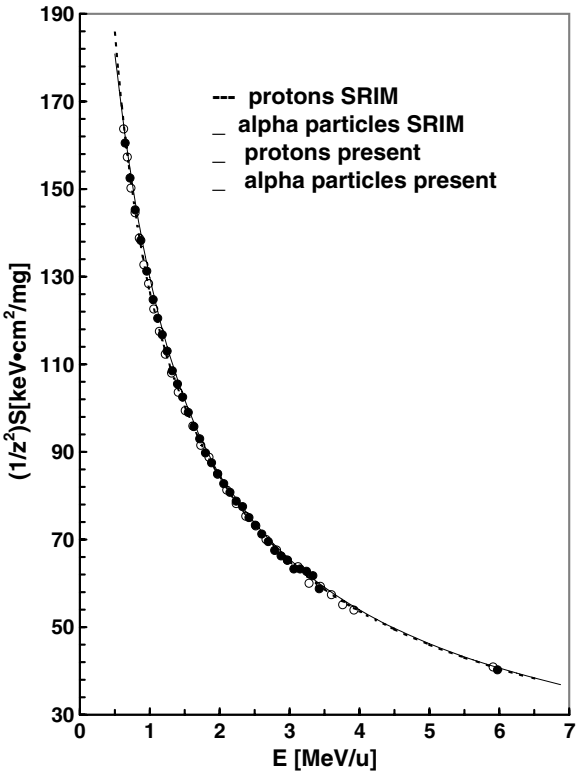

Figure 3. Results of current measurements for protons (open triangles) and alpha particles (open circles) traversing havar target foils, compared with SRIM 2003 predictions for protons (dashed curve) and alpha particles (solid curve).

Table 6. The mean excitation energy (I) with associated uncertainty (ΔI) and Barkas-effect parameter (b) with associated uncertainty (Δb) for proton and alpha particle projectiles traversing a havar target.

Projectile	$I \pm \Delta I$ (eV)	$b \pm \Delta b$
Protons	304.3 ± 2.4	1.37 ± 0.04
Alpha particles	306.3 ± 2.3	1.47 ± 0.03

6. Summary and conclusions

The stopping powers of havar for 0.63–5.9 MeV protons and 2.6–24 MeV alpha particles have been measured with a new method [10, 13]. Analysis of these measurements in terms of modified Bethe–Bloch theory has provided the opportunity to extract values of the two most important parameters of the formalism, the mean excitation energy (I) and the Barkas-effect parameter (b). The projectile energy intervals selected for analysis were sufficiently high as to preclude the need for inclusion of any effective charge parameters.

Results of the current study were compared with those previously obtained for measurements with the same projectile–target combinations, but over much narrower projectile energy intervals [4]. Those data, taken for 0.5–2.4 MeV protons and 1.2–1.8 MeV alpha particles with an accuracy close to 0.6%, yielded parameter values in reasonable agreement with the current results. The current measurements feature relative uncertainties between 1.4 and 2.3% for protons, and between 1.1 and 1.5% for alpha particles, as shown in tables 2 and 3, respectively.

Another feature of interest in the results of the current study pertains to the existence of trends in extracted I- and b-values with increasing projectile z-value, wherein I-values increase and b-values decrease [5, 11, 34–39]. In the values displayed in table 6 the observed trend in b-values is followed, whereas the extracted I-values are consistent with the observed trend in the sense of overlapping ranges of values provided by the uncertainties.

References

[1] ICRU 1993 Stopping Power and Ranges for Protons and Alpha Particles *ICRU Report No 49* (Bethesda, MD: ICRU)
[2] Porter L E 1994 *Phys. Rev.* A **50** 2397
[3] Porter L E 1999 *Nucl. Instrum. Methods* B **159** 195
[4] Porter L E, Rauhala E and Räisänen J 1994 *Phys. Rev.* B **49** 11543
[5] Porter L E, Räisänen J and Munnik F 2002 *Int. J. Quantum Chem.* **90** 1368
[6] Bragg W H and Kleeman R 1905 *Phil. Mag.* **10** 318
[7] Porter L E and McIntyre L C 1964 *Energy Loss in Havar Foils* (Madison, WI: University of Wisconsin) p 16, unpublished
[8] Porter L E, McIntyre L C and Haeberli W 1970 *Nucl. Instrum. Methods* **89** 237
[9] Porter L E 1991 *Radiat. Eff. Defects Solids* **117** 197
[10] Trzaska W H, Lyapin V, Alanko T, Mutterer M, Räisänen J, Tjurin G and Wojdyr M 2002 *Nucl. Instrum. Methods* B **195** 147
[11] Räisänen J, Trzaska W H, Alanko T, Lyapin V and Porter L E 2003 *J. Appl. Phys.* **94** 2080
[12] Räisänen J and Rauhala E 1989 *Radiat. Eff. Defects Solids* **108** 21
[13] Trzaska W H, Alanko T, Lyapin V and Räisänen J 2001 *Nucl. Instrum. Methods* B **183** 203
[14] Bradley M, private communication
[15] Porter L E and Lin H 1990 *J. Appl. Phys.* **67** 6613
[16] Ashley J C, Ritchie R H and Brandt W 1972 *Phys. Rev.* B **5** 2393
[17] Ashley J C, Ritchie R H and Brandt W 1973 *Phys. Rev.* A **8** 2402
[18] Ashley J C 1974 *Phys. Rev.* B **9** 334
[19] Ritchie R H and Brandt W 1978 *Phys. Rev.* A **17** 2102
[20] Bloch F 1933 *Ann. Phys., Lpz.* **16** 285
[21] Lindhard J 1976 *Nucl. Instrum. Methods* **132** 1
[22] Abramowitz M and Stegun I A (ed) 1964 *Handbook of Mathematical Functions* (Washington, DC: National Bureau of Standards) p 259
[23] Pitarke J M, Ritchie R H and Echenique P M 1995 *Phys. Rev.* B **52** 13883
[24] Walske M C 1952 *Phys. Rev.* **88** 1283
[25] Walske M C 1956 *Phys. Rev.* **101** 940
[26] Sternheimer R M, Berger M J and Seltzer S M 1984 *At. Data Nucl. Data Tables* **30** 261
[27] Jackson J D and McCarthy R L 1972 *Phys. Rev.* B **6** 4131
[28] Porter L E 1987 *Radiat. Res.* **110** 1
[29] Fano U 1963 *Annu. Rev. Nucl. Sci.* **13** 1
[30] Fermi E 1940 *Phys. Rev.* **57** 485
See also Uehling E 1954 *Annu. Rev. Nucl. Sci.* **4** 315
[31] Fano U 1956 *Phys. Rev.* **103** 1202
[32] Barkas W H and Berger M J 1967 Studies in penetration of charged particles in matter *National Academy of Sciences–National Research Council Publication* No. 1133 (Washington, DC: NAS-NRC)
[33] Ziegler J F 2003 *Computer Code SRIM*
[34] Porter L E 2000 *Proc. 20th Werner Brandt Workshop on Penetration Phenomena (Feb. 2000)* ed J R Sabin (Gainesville, FL: University of Florida)
[35] Porter L E 2002 *Int. J. Quantum Chem.* **90** 684
[36] Porter L E 2003 *J. Electron Spectrosc.* **129** 273
[37] Porter L E 2003 *Int. J. Quantum Chem.* **95** 504
[38] July Porter L E 2004 *Adv. Quantum Chem.* **46** 91
[39] Porter L E 2004 *Int. J. Quantum Chem.* at press